JOURNAL OF MATERIALS SCIENCE: MATERIALS IN MEDICINE **11** (2000) 601–608

Comparison of mechanical properties for equiaxed fine-grained and dendritic high-palladium alloys

E. PAPAZOGLOU[1], Q. WU[2], W. A. BRANTLEY[1], J. C. MITCHELL[3], G. MEYRICK[4]
[1]College of Dentistry, [2]Therm-O-Disc, Inc., Mansfield, OH, USA, [3]Department of Geological Sciences and [4]Department of Materials Science and Engineering, The Ohio State University, Columbus, OH, USA
E-mail: Papazoglou.1@osu.edu

Two Pd-Cu-Ga alloys and a Pd-Ga alloy were selected for study. Bars of each alloy were tested in tension for the as-cast and simulated porcelain-firing conditions, and values of mechanical properties were measured. Fracture surfaces and microstructures of axially sectioned fracture specimens were observed with the SEM. The two Pd-Cu-Ga alloys exhibited similar mechanical properties. The Pd-Ga alloy had lower strength and higher percentage elongation. Heat treatment simulating porcelain firing cycles decreased the strength of both Pd-Cu-Ga alloys and increased their ductility. However, this heat treatment did not significantly affect the mechanical properties of the Pd-Ga alloy. All three high-palladium alloys had the same modulus of elasticity. The amount of overall porosity was relatively minimal ($<1\%$) and not significantly different among the three alloys. However, porosity was a significant factor for UTS of one Pd-Cu-Ga alloy and the Pd-Ga alloy.
© *2000 Kluwer Academic Publishers*

1. Introduction

The original group of Pd-Cu-Ga dental casting alloys that were introduced in the market in the early 1980s lacked grain-refining elements (typically ruthenium) and had a dendritic as-cast microstructure [1–4]. Addition of ruthenium gave an eqiaxed fine-grained microstructure [2, 5, 6].

The original Pd-Cu-Ga alloys presented high levels of hardness and yield strength, which might cause problems during finishing and polishing of cast restorations [1]. Additionally, their marginal creep was questioned, based upon the results of high-temperature three-point bending experiments under varying stresses [7]. It has also been shown that some Pd-Cu-Ga alloys are difficult to mask for metal-ceramic restorations, and that sometimes a thicker opaque porcelain layer is required to avoid low value (i.e. undesired darkness) with certain porcelain systems [8–10]. Moreover, some concerns were expressed about the biocompatibility of the Pd-Cu-Ga alloys; however, these concerns were never scientifically substantiated [11]. As a solution to these problems, the Pd-Ga alloys with small amounts of Ag were developed [1].

Lamellar eutectic microstructures have been observed in Pd-Cu-Ga alloys and interpreted [1, 2, 12–15] as consisting of Pd_2Ga and the palladium solid solution, based on the Pd-Ga phase diagram. For the compositions of the high-palladium alloys, Cu and In components reduce the solubility of Ga in Pd [16]. Along with rapid solidification of the alloys under dental casting conditions, this results in increased percentages of the eutectic constituent in the microstructure, particularly near the surface and in thin sections of castings where the solidification is most rapid [1, 2].

Heat treatment simulating the porcelain firing cycles caused significant microstructural changes for some Pd-Cu-Ga alloys selected for study [1, 2]. The dendritic microstructure and the lamellar eutectic structure disappeared, and there was substantial homogenization of the overall elemental composition within the grains of the bulk structure. In contrast to these Pd-Cu-Ga alloys, simulated porcelain-firing heat treatment caused much smaller changes in the two Pd-Ga alloys studied, which had equiaxed as-cast microstructures without a eutectic constituent [1, 2].

The effect of heat treatment on the hardness of these selected high-palladium alloys has also been previously studied. The as-cast and simulated porcelain firing conditions have been compared, and heat treatments have been performed at specific temperatures spanning the porcelain firing cycles [2–4, 15, 17, 18]. The largest decreases in hardness were observed for the Pd-Cu-Ga alloy containing substantial eutectic structure in the as-cast condition [2–4, 15, 17, 18].

The objectives of this investigation were to determine a wider variety of mechanical properties for three previously studied high-palladium alloys (two Pd-Cu-Ga alloys and one Pd-Ga alloy) cast under standard

Address for correspondence and reprint requests to: Efstratios Papazoglou, DDS, MS, PhD, Assistant Professor, Section of Restorative Dentistry, Prosthodontics and Endodontics, College of Dentistry, The Ohio State University, 305 West 12th Avenue, Room 3001-C, Columbus, OH 43210-1241, USA

0957–4530 © *2000 Kluwer Academic Publishers*

dental laboratory conditions. These mechanical properties were compared to the previous Vickers hardness measurements that had been used to make conclusions about the relative strength properties of the alloys. Additionally, the effect of heat treatment simulating the porcelain firing cycles on the mechanical properties was investigated.

2. Materials and methods

2.1. Materials and preparation of tensile test bars

Three high-palladium alloys were selected for study. Spartan Plus (Williams/Ivoclar Amherst, NY) is an Option-like alloy with a nominal composition of 79% Pd, 10% Cu, 9% Ga and 2% Au, and a dendritic as-cast microstructure [1, 2]. Liberty (J.F. Jelenko & Co., Armonk, NY) has a nominal composition of 76% Pd, 10% Cu, 5.5% Ga, 6% Sn, 2% Au, and a small amount of Ru (less than 1%). Protocol (Williams/Ivoclar) is a Cu-free high-palladium alloy with a nominal composition of 75% Pd, 6% Ga, 6% In, 6.5% Ag, and 6% Au, and also contains less than 1% Ru. Both Liberty and Protocol have equiaxed fine-grained as-cast microstructures [1, 2].

Cast bars of each alloy were tested in tension for both the as-cast and simulated porcelain-firing conditions. Six specimens of approximately 3-mm diameter were cast for each alloy and condition; all metal used for each alloy came from the same batch. Polystyrene plastic patterns (Salco, Romeoville, IL, USA) that satisfy the dimensional requirements in ANSI/ADA specifications no. 5 [19] and 38 [20] were used, and each specimen was sprued in a horizontal configuration to minimize the casting porosity [21]. Each pattern was invested in a separate casting ring, and a carbon-free, phosphate-bonded investment (Cera-Fina, Whip-Mix, Louisville, KY, USA) was employed with a two-stage burn-out procedure and a peak temperature of 1088 K. One-half of a Troy ounce (10 dwt) of alloy was used for each pattern, producing buttonless castings. It has been shown that satisfactory three-unit bridges [22, 23] and removable partial dentures [24] are obtained from buttonless castings. A multi-orifice torch with 5 psi gas (bottled liquid petroleum) and 10 psi oxygen pressures was utilized to melt the alloys, following recommendations in the Williams/Ivoclar product information literature.

Casting was performed in air under standard dental laboratory conditions, using a conventional broken-arm centrifugal casting machine (Kerr/Sybron, Romulus, MI, USA) and a dedicated ceramic crucible for each alloy. All castings were bench-cooled, following the standard manufacturer recommendations. After devesting, the sprues and any visible nodules or fins on the surfaces were removed with a carborundum separating disk. No air abrasion or polishing was performed on the cast bars, and no specimens were discarded because of visible shrinkage defects or porosities. The heat-treated specimens received the recommended firing cycles for Vita VMK 69 porcelain (Vident, Baldwin Park, CA, USA). Each firing cycle for the opaque porcelain, body porcelain and glaze involved heating the alloy from approximately 923 to over 1173 K during an 8–10 min period [25].

2.2. Mechanical properties

Prior to testing, the diameter for each bar specimen was measured with a digital micrometer (Mitutoyo, Shiwa, Japan). A sharp razor blade was used to mark the central 15-mm gauge section for the determination of percentage elongation. Specimens were loaded with a screw-driven mechanical testing machine (Model 4204, Instron Corporation, Canton, MA, USA), using a crosshead speed of 0.5 mm/min. Custom-fabricated grips, prepared by grinding the interiors of two Jacobs chucks [26], provided self-aligning capability during tensile loading [27]. A strain gauge extensometer attached to the specimen recorded the elongation over the central 10-mm length.

The elongation, load and crosshead position were recorded by a personal computer (PC), using the software program LabVIEW (National Instruments, Austin, TX, USA) for Windows and a data acquisition card. The position of the crosshead, and the values of the elongation and load, were also observed graphically during each tension test with the PC monitor. Each tension test was interrupted before the elongation reached 1 mm or 10%, and the extensometer (maximum allowable elongation of 10%) was removed; then the specimen was further loaded to fracture. The software program Excel (Microsoft Corporation, Redmond, WA, USA) was used to generate graphs of engineering stress versus strain from the raw test data.

Standard relationships were used to calculate the engineering stress and strain and Young's modulus (E) from the applied load, initial cross-section area, elongation and original gauge length. The ANSI/ADA specification no. 5 for dental casting alloys [19] requires calculation of the 0.1% yield strength (0.1% YS), while the ANSI/ADA specification no. 38 for metal-ceramic systems [20] requires measurement of the 0.2% yield strength (0.2% YS). These yield strengths were obtained in the usual manner from the offsets of 0.001 (0.1%) or 0.002 (0.2%) on the strain axis. The ultimate tensile strength (UTS), i.e. the maximum value of stress applied to the specimen, was determined directly from the raw data stored by the testing machine.

The work-hardening characteristics of the alloys in the permanent deformation range were determined between the 0.1% YS and UTS, using the power–law relationship: $\sigma = K\varepsilon^n$, where the constants n and K are the strain-hardening exponent and the strength coefficient, respectively [28]. Here σ and ε are the true stress and true strain, respectively, which are related to the engineering stress (s) and strain (e) by the following equations: $\sigma = s(1+e)$ and $\varepsilon = ln\ (1+e)$ [28]. When logarithms are taken of both sides of the power-law equation, the slope of the resulting straight line is n and the intercept on the vertical axis is ($ln\ K$). Once necking occurs at the UTS, the power-law relationship does not apply, since strains and stresses are no longer uniform over the gauge length.

2.3. Examination of fracture surfaces and measurement of percentage elongation

Fracture surfaces for each test specimen were examined with a scanning electron microscope (SEM) (JSM-820, JEOL Ltd, Tokyo, Japan) to assess the relative ductile or brittle character and gain insight into the role of porosity and other casting defects for fracture initiation. In particular, evidence for dimpled rupture characteristic of ductile fracture [28] in wrought dental alloys [29] was sought. Specimens were not cleaned ultrasonically before observation, in order to retain particles within microvoids and to not lose evidence of secondary microstructural phases on the fracture surfaces. After SEM examination, the percentage elongation was obtained from the permanent change in the gauge length. Measurements were made with the aid of a traveling microscope (Measurescope MM-11, Nikon, Tokyo, Japan) after carefully fitting together the two fractured portions of each specimen.

2.4. Statistical analysis of mechanical property data

Two-way analysis of variance (ANOVA) and the Tukey-Kramer HSD test ($\alpha = 0.05$) were employed for statistical analysis of the data, using a software package (SPSS, Chicago, IL, USA). Each of the mechanical properties (E, 0.1% YS, 0.2% YS, UTS and percentage elongation) for the three alloys were compared for the as-cast and heat-treated conditions.

2.5. Measurement of casting porosity and examination of microstructures

The smaller portions of the fractured test bars for each alloy were mounted in metallographic resin (Epoxide, Leco Corporation, St. Joseph, MI, USA) and sectioned parallel to the axis, using a slow-speed water-cooled diamond saw (Vari/Cut VC-50, Leco Corporation). After metallographic polishing through 0.05-μm alumina slurries, the cross-sections were examined in an optical microscope at X50 magnification for the presence of porosity and other casting defects. Quantitative metallographic techniques [30] using computerized image analysis software (Omnimet®, Buehler Corporation, Lake Bluff, IL, USA) were employed to analyze the porosity in the test bars. Ten measurements were made from near the site of fracture to near the gripped end for each test specimen. Analysis of covariance (JMP IN, SAS Institute, Cary, NC, USA) was employed to search for a relationship between UTS (dependent variable) and total amount of casting porosity (independent variable) for each alloy and condition.

Polished cross-sections of the fractured test bars were also etched with aqua regia [1, 2] and observed with the SEM. This was deemed essential to correlate the fracture surface topography with the size and distribution of the microstructural constituents, since the fracture surface might not be representative of the true alloy microstructure.

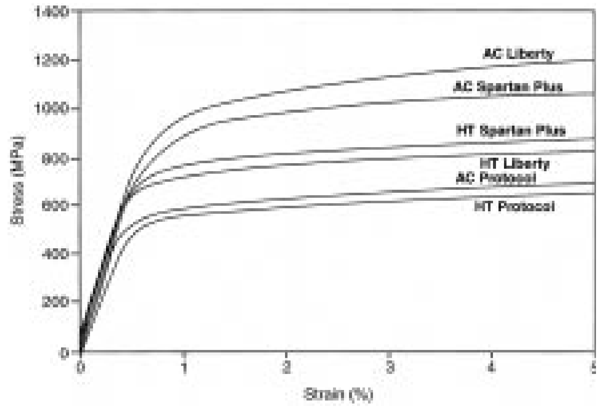

Figure 1 Representative engineering tensile stress-strain curves for the three high-palladium alloys. All curves were truncated at 5% strain. (AC = as-cast and bench-cooled; HT = heat treatment simulating the porcelain firing cycles.)

3. Results

3.1. Mechanical properties

Representative engineering stress-strain curves of the three alloys in the as-cast and heat-treated conditions appear in Fig. 1.

The results of the two-way ANOVA tests for each of the mechanical properties are shown in Table I. It was found that for the variable (alloy) there were significant differences for the 0.1% YS, 0.2% YS, UTS, percentage elongation, n and K. For the variable (condition) there were significant differences for the 0.1% YS, 0.2% YS, percentage elongation and K. Finally, there were significant interactions between (alloy) and (condition) for 0.1% YS, 0.2% YS, UTS, percentage elongation and K.

Values (mean $\pm$ SD) of all mechanical properties are given in Table II. The groups with the same letter that belong to the same column in Table II are not significantly different ($P > 0.05$). Other than E, significant differences were typically found in mechanical properties for the different alloys and conditions. For 0.1% YS, 0.2% YS and UTS, as-cast Spartan Plus and Liberty had the highest values, followed by the same two alloys in the heat-treated conditions. There was no significant difference in the values of UTS for heat-treated Spartan Plus and as-cast Spartan Plus and Liberty, and between heat-treated Liberty and as-cast and heat-treated Protocol. The 0.1% YS, 0.2% YS and UTS for

TABLE I Two-way ANOVA results for mechanical properties

Independent variable	0.1% YS	0.2% YS	UTS	Percentage elongation	E	n	K
Alloy	$P < 0.0001$ Significant	$P < 0.0001$ Significant	$P < 0.0001$ Significant	$P < 0.0001$ Significant	$P = 0.2237$ Not significant	$P = 0.0002$ Significant	$P < 0.0001$ Significant
Condition	$P < 0.0001$ Significant	$P < 0.0001$ Significant	$P = 0.0512$ Not significant	$P < 0.0001$ Significant	$P = 0.7284$ Not significant	$P = 0.6614$ Not significant	$P < 0.0001$ Significant
Alloy* Condition Interaction	$P < 0.0001$ Significant	$P < 0.0001$ Significant	$P = 0.0228$ Significant	$P = 0.0126$ Significant	$P = 0.7890$ Not significant	$P = 0.5173$ Not significant	$P = 0.0003$ Significant

TABLE II Mechanical properties of the alloys Spartan Plus (S), Liberty (L) and Protocol (P) in the as-cast (AC) and heat-treated (HT) conditions. Groups in the same column with the same letters are not significantly different ($P > 0.05$)

Alloy/Condition	0.1% YS(MPa)	0.2% YS(MPa)	UTS(MPa)	Elongation(%)	E(GPa)	*n*	K(MPa)
S (AC)	791 ± 29 A	851 ± 31 A	1075 ± 71 A	8.7 ± 4.8 CD	133 ± 15 A	0.14 ± 0.03 AB	1773 ± 271 A
S (HT)	700 ± 13 B	725 ± 9 B	1002 ± 9 AB	24.1 ± 1.5 B	141 ± 28 A	0.11 ± 0.00 B	1271 ± 16 B
L (AC)	822 ± 51 A	872 ± 45 A	1078 ± 95 A	6.0 ± 2.8 D	131 ± 22 A	0.15 ± 0.03 A	1821 ± 193 A
L (HT)	673 ± 36 B	689 ± 35 B	902 ± 123 BC	16.0 ± 10.0 BC	130 ± 16 A	0.12 ± 0.00 AB	1202 ± 56 BC
P (AC)	534 ± 5 C	552 ± 4 C	770 ± 145 C	35.2 ± 2.9 A	123 ± 18 A	0.14 ± 0.01 AB	1085 ± 53 BC
P (HT)	532 ± 10 C	547 ± 8 C	824 ± 71 C	36.2 ± 2.8 A	123 ± 15 A	0.12 ± 0.00 AB	996 ± 21 C

Protocol were not significantly different for the as-cast and heat-treated conditions. This alloy was weaker than Spartan Plus and Liberty, except for the UTS not being significantly different from that for heat-treated Liberty, and had the highest percentage elongation. The lowest percentage elongation values were obtained for the strongest alloys, as-cast Liberty and Spartan Plus; however, the percentage elongation values for as-cast Spartan Plus and heat-treated Liberty were not significantly different. Heat treatment lowered the value of K for all three alloys, although the decrease was not statistically significant for Protocol.

3.2. SEM examination of fracture surfaces

SEM examination of the fracture surfaces for as-cast Spartan Plus at low magnification showed the dendritic microstructure (Fig. 2). The presence of a few dimples at higher magnification (Fig. 3) was indicative of some ductile fracture in this alloy. The regions containing microvoids were presumably the palladium solid solution dendrites, since the interdendritic regions that contain multiple phases [2] should undergo a more brittle mode of fracture. Heat-treated Spartan Plus specimens had fracture surfaces consisting almost entirely of dimples, along with some small voids that appeared to be casting porosity. It was found that heat treatment of Spartan Plus largely eliminated the as-cast dendritic microstructure in the tension test specimens, as was previously found for small castings simulating a coping for a maxillary central incisor [2, 3, 17, 18].

The fracture surfaces of as-cast Liberty contained dimples, embedded particles, casting porosity and regions of incomplete grain formation during solidification. Their appearance suggested a mixture of ductile and brittle fracture processes (Figs 4–6). There was no evidence of the previously reported [1, 2, 4, 14] fine-scale lamellar eutectic constituent at the fracture surface. Heat-treated specimens showed substantial ductile fracture, evidenced by the dominant presence of dimples.

The as-cast Protocol fracture surfaces contained extensive amounts of the dimples associated with ductile fracture (Fig. 7), and larger surface features corresponded approximately to the reported [1, 2] 15–25 μm grain size of the alloy. Substantial amounts of casting porosity and regions of incomplete formation of grains in as-cast Protocol can be seen in Fig. 8. These latter regions may correspond to localized dendritic solidification arising from depletion of the grain-refining element ruthenium. The fracture surface for the heat-treated Protocol specimen in Fig. 9 contains a large number of fine-scale dimples and substantial porosity.

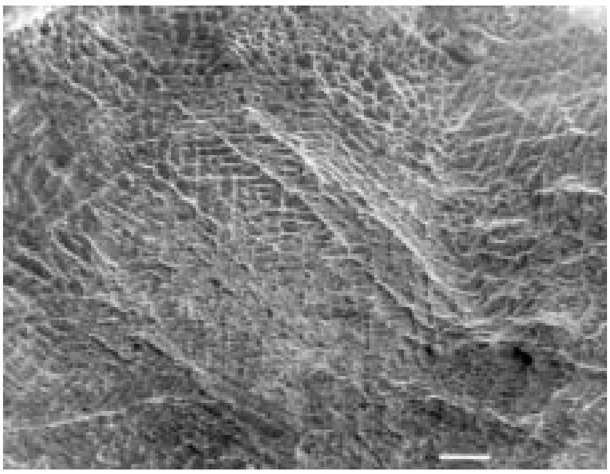

Figure 2 Low-magnification scanning electron micrograph of the tensile fracture surface for an as-cast Spartan Plus specimen. An overall dendritic microstructure is evident. Bar = 100 μm.

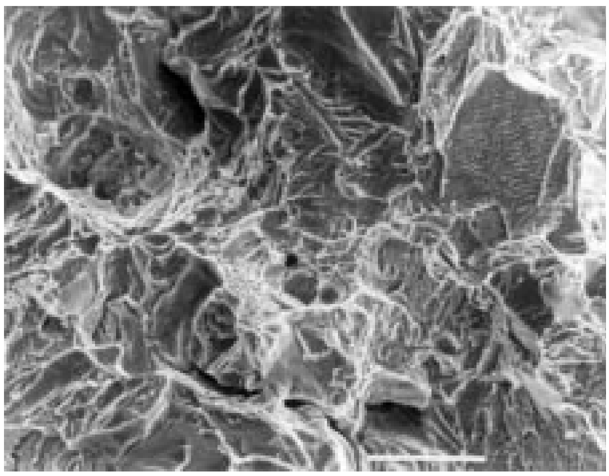

Figure 3 High-magnification scanning electron micrograph of the tensile fracture surface for an as-cast Spartan Plus specimen. Secondary phase particles and dimples are evident. Bar = 10 μm.

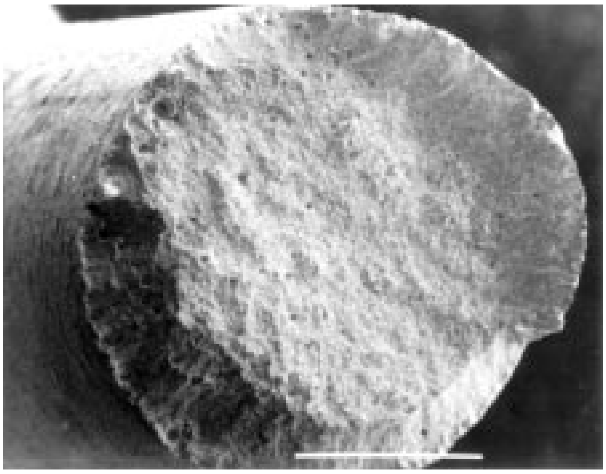

Figure 4 Low-magnification scanning electron micrograph of the tensile fracture surface for an as-cast Liberty specimen. Prominent shear lips (typically all fractured specimens) and some casting porosity can be seen. Bar = 1 mm.

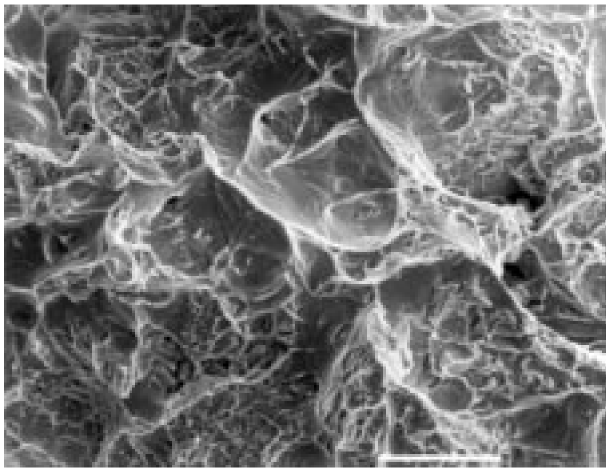

Figure 6 High-magnification scanning electron micrograph of the tensile fracture surface for an as-cast Liberty specimen, showing dimples and embedded particles. The larger-scale features on the fracture surface appear to correspond to the 15–25 μm grain size [1, 2] of this alloy. Bar = 10 μm.

3.3. Porosity and microstructures of sectioned specimens

From the image analysis of unpolished, axially-sectioned fractured specimens of as-cast alloys, the total porosity for Spartan Plus was $0.11 \pm 0.12\%$, while it was $0.85 \pm 1.48\%$ for Liberty and $0.83 \pm 1.05\%$ for Protocol. Analysis of variance showed no significant difference among the mean values of the relatively minimal bulk porosity in the three alloys. Linear regression analysis indicated that porosity was a significant factor for the UTS of Liberty ($P = 0.05$) and Protocol ($P = 0.003$), but not for Spartan Plus ($P = 0.384$). The coefficients of determination (r^2) were 0.66 for Liberty, 0.91 for Protocol and 0.19 for Spartan Plus (Fig. 10).

SEM examination of polished and etched, axially-sectioned, fractured specimens verified that heat treatment eliminated the dendritic structure of as-cast Spartan Plus (Fig. 11). The crystallographic appearance of some linear microstructural features in this figure suggests that twinning has occurred. Examination of the sectioned specimens also confirmed that the as-cast tensile test specimens of Liberty did not contain a near-surface eutectic constituent. The microstructure of heat-treated Liberty contained small amounts of a grain-boundary phase assumed to be Pd_5Ga_2 and a network of grain-boundary precipitates assumed to be Pd_2Ga [31] (Fig. 12). Cracks perpendicular to the surface of the tensile test bar were observed for heat-treated Spartan Plus and Liberty. These cracks extended approximately to the boundary of the subsurface oxidation layer with the bulk alloy, and occasionally deflected and propagated horizontally in the subsurface oxidation region (Fig. 13).

4. Discussion

4.1. Mechanical properties

The modulus of elasticity (E) is not significantly different for the three alloys in either the as-cast or heat-treated conditions (Table II). This result was expected, since E depends on binding forces between atoms [28].

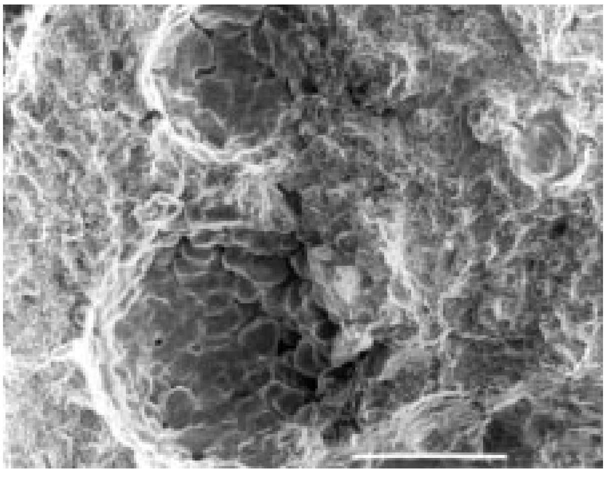

Figure 5 Scanning electron micrograph of the tensile fracture surface for an as-cast Liberty specimen, showing incomplete formation of grains inside large pores near the specimen edge. There was no evidence of a fine-scale lamellar eutectic constituent. Bar = 100 μm.

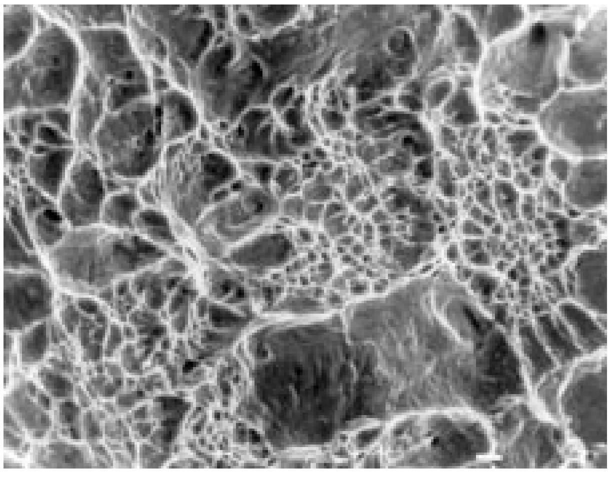

Figure 7 High-magnification scanning electron micrograph of the tensile fracture surface for an as-cast Protocol specimen, showing dimples and embedded particles. Bar = 1 μm.

TABLE III Mechanical properties of the alloys Spartan Plus (S), Liberty (L) and Protocol (P) for the as-cast (AC) and heat-treated (HT) conditions from other publications and product information literature

Alloy/condition	0.1% YS (MPa)	0.2% YS (MPa)	UTS (MPa)	Elongation (%)	E (GPa)	Vickers Hardness
S (AC)*						354
S (HT)*						296
L (AC)§						334
L (HT)§						285
P (AC)§						253
P (HT)§						242
S (HT)†	634	795		20	97	310
L (HT)†	797 (not specified if 0.1 or 0.2% YS)	1144	14			
P (HT)†	474	500		34	103	

* From [17, 18]. § From [3]. † From product information literature.

Moreover, although there are composition differences among the alloys, transmission electron microscopic observations by Cai *et al*. [32] have shown that the ultrastructures of the three undeformed alloys in the present study are very similar for both the as-cast and heat-treated conditions. Variations in elastic modulus values shown in Table II result from inherent accuracy limitations in the technique used.

Although heat treatment does not change the basic interatomic bonding, it alters the microstructures of the two Pd-Cu-Ga alloys studied [2–4, 15, 17, 18, 31]. For these alloys, the significant decreases in 0.1% YS, 0.2% YS and UTS might be attributed to the disappearance of hard secondary phases in the interdendritic areas for Spartan Plus and the reduction or elimination of the hard grain-boundary Pd_5Ga_2 phase for Liberty [15, 17, 18, 31]. The percentage elongation of Protocol was higher than for the other two alloys and was not affected by heat treatment, despite the reported [2] microstructural homogenization of this alloy following heat treatment simulating the porcelain firing cycles. The percentage elongation at fracture of Spartan Plus and Liberty was greatly increased after heat treatment. This was attributed to the elimination of the dendritic microstructure for Spartan Plus and transformation of the hard phase [18, 31], which acts as a barrier for dislocation movement, in both alloys.

The present results concur with some previous findings for Vickers hardness [3, 4, 17, 18], where heat treatment significantly softened the two Pd-Cu-Ga alloys compared to the as-cast condition (Table III). The Pd-Ga alloy Protocol that had been previously shown to exhibit significantly lower hardness after heat treatment [3] was not weakened by heat treatment in this study (Table II). However, Table III shows that the previously reported statistically significant difference in Vickers hardness for as-cast and heat-treated Protocol has little practical significance.

The clinically acceptable level for each mechanical property is not well established. In ANSI/ADA specification no. 38 [20], there is a lower-limit requirement of 250 MPa for 0.2% YS and a minimum acceptable value of 2% elongation for alloys that will be bonded to dental porcelain. In ANSI/ADA specification no. 5 [19], there are lower-limit requirements for Type IV casting alloys for fixed prosthodontics of 340 MPa for 0.1% YS in the softened (annealed) condition and 500 MPa in the hardened (heat-treated) condition, along with a minimum value of 2% elongation. Table II shows that the Pd-Cu-Ga and Pd-Ga alloys selected for study have yield

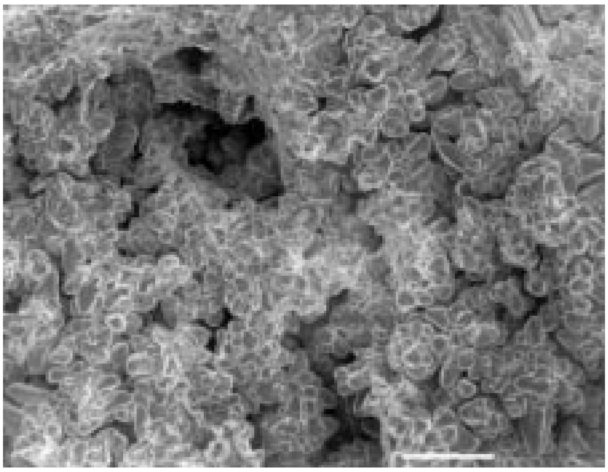

Figure 8 Low-magnification scanning electron micrograph of the tensile fracture surface for an as-cast Protocol specimen, showing incomplete formation of grains and some very large pores. Dimples were not found in these areas. Bar = 100 μm.

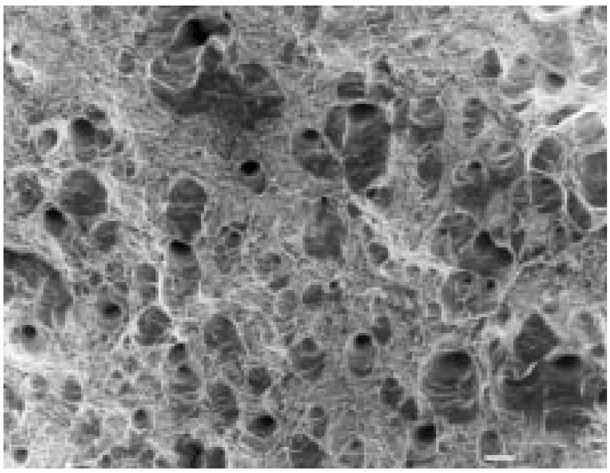

Figure 9 Scanning electron micrograph of the tensile fracture surface for a heat-treated Protocol specimen, showing a very large number of fine-scale dimples and substantial porosity. The features on the fracture surface appear to correspond approximately to the 15–25 μm grain size previously reported [1, 2] for this alloy. Bar = 10 μm.

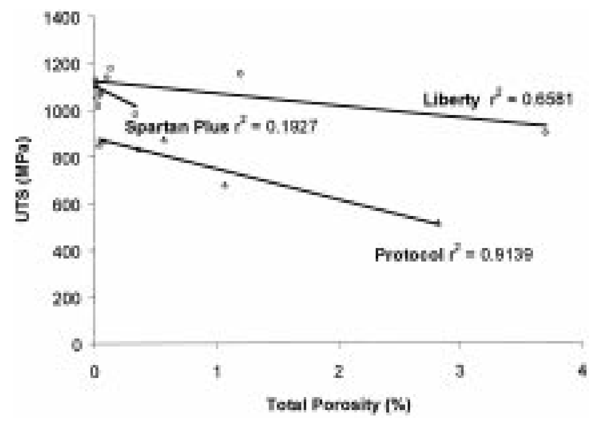

Figure 10 Regression lines and coefficients of determination (r^2) for relationships between UTS and the percentage of total porosity for the three alloys.

strength and percentage elongation values above the lower limits empirically set in the two ANSI/ADA specifications.

It should also be noted that, since the Pd-Ga alloy has the same elastic modulus as the two Pd-Cu-Ga alloys, it is expected that this alloy will resist deformation up to its yield strength in the same manner as will the Pd-Cu-Ga alloys. It is not expected that masticatory forces will induce stress levels in cast dental restorations that will exceed the 500 MPa limit for 0.1% YS found in ANSI/ADA specification no. 5. Consequently, all three high-palladium alloys studied should adequately resist intraoral forces without undergoing permanent deformation. For long term clinical success, fatigue strength is more important, since cyclic loading conditions occur *in vivo*, and this property is currently being investigated for the high-palladium alloys.

4.2. Microstructures and porosity

As observed in previous studies [1–4, 17, 18] the as-cast dendritic microstructure of Spartan Plus was nearly eliminated by simulated porcelain firing heat treatment, and new phases were observed. An interesting result was the apparent absence of a near-surface eutectic constituent in as-cast Liberty that had been observed in thin sections of much smaller castings [1, 2, 4, 14]. This is attributed to the much lower solidification rate of the cast specimens for the tensile test, which resulted in substantially smaller shift of the eutectic point to higher percentages of palladium [2]. Microstructures of heat-treated Liberty, and both as-cast and heat-treated Protocol, were consistent with previous studies [1, 2].

The cracks observed in the oxidation area of the fractured, heat-treated Liberty specimens (Fig. 13) demonstrate the relatively weak and brittle nature of this region, which would be anticipated. Further research is necessary to determine whether this crack propagation has clinical significance for the failure of metal-ceramic restorations.

A relatively small amount of porosity was found in the castings of all three alloys, when the polished, axially-

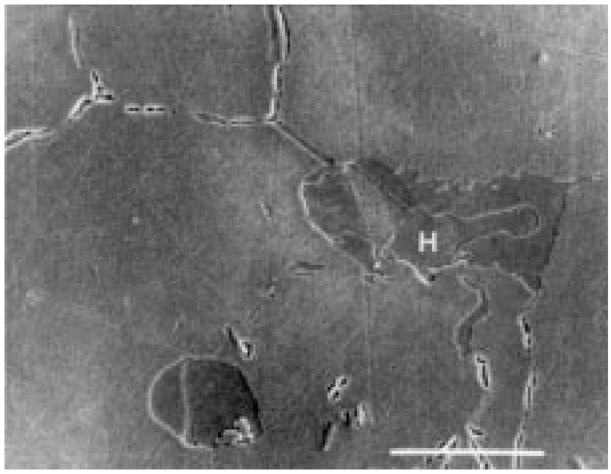

Figure 12 High-magnification scanning electron micrograph of a polished and etched, axially-sectioned, heat-treated Liberty specimen after fracture, showing the hard Pd_5Ga_2 phase (H) and small grain boundary precipitates assumed to be Pd_2Ga. Bar = 10 μm.

Figure 11 Scanning electron micrograph of a polished and etched, axially-sectioned, as-cast Spartan Plus specimen after fracture, showing crystallographic features in the palladium solid solution suggestive of twinning. A lamellar eutectic constituent in the interdendritic region is evident at higher magnification. Bar = 100 μm.

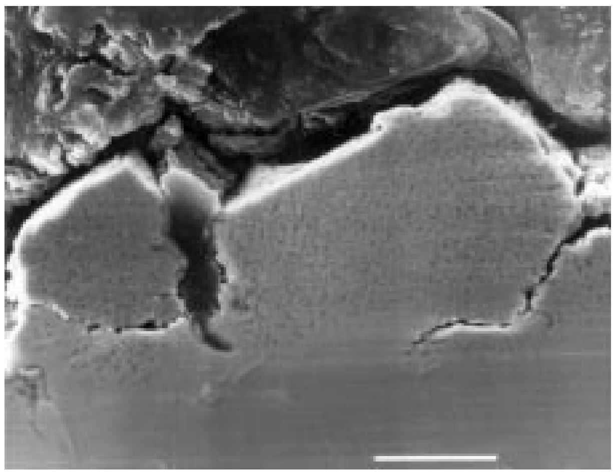

Figure 13 High-magnification scanning electron micrograph of a polished and etched, axially-sectioned, heat-treated Liberty specimen after fracture, showing cracks that extend to the boundary of the subsurface oxidation layer. Bar = 10 μm.

sectioned, fractured specimens were examined. This result is in accord with a previous study of a Pd-Ga alloy, where minimal porosity was found in similar specimens fabricated by induction melting and centrifugal casting [33]. Therefore, it appears that torch-melting of these high-palladium alloys for large patterns produces castings of acceptable quality for both Pd-Cu-Ga and Pd-Ga alloys. However, as found in a recent study on the mechanical properties of a remelted gold alloy [34], fracture of cast specimens during tensile loading typically occurs at sites where there is casting porosity. Evidence of this deleterious role of casting porosity can be seen in Figs. 4, 5, 8 and 9, and is assumed to account for the significant dependences of UTS on porosity for Liberty and Protocol.

5. Conclusions

Under the conditions of the study, the following conclusions may be made:

1. The two Pd-Cu-Ga alloys, Spartan Plus and Liberty, exhibited similar mechanical properties. The Pd-Ga alloy Protocol had lower strength and higher percentage elongation.
2. Heat treatment simulating porcelain firing cycles decreased the strength of both Pd-Cu-Ga alloys and increased their ductility. However, this heat treatment did not significantly affect the mechanical properties of the Pd-Ga alloy.
3. All three high-palladium alloys had the same modulus of elasticity.
4. The amount of overall porosity was relatively minimal ($< 1\%$) and not significantly different among the three high-palladium alloys. However, porosity was a significant factor for UTS of the Liberty and Protocol alloys, because fracture occurred at sites where occasional large pores or clusters of porosity were located.

Acknowledgment

Support was received from Grant DE10147, National Institute of Dental and Craniofacial Research, Bethesda, MD, USA.

References

1. A. B. CARR and W. A. BRANTLEY, *Int. J. Prosthodont.* **4** (1991) 265.
2. W. A. BRANTLEY, Z. CAI, A. B. CARR and J. C. MITCHELL, *Cells Mater.* **3** (1993) 103.
3. A. B. CARR, Z. CAI, W. A. BRANTLEY and J. C. MITCHELL, *Int. J. Prosthodont.* **6** (1993) 233.
4. W. A. BRANTLEY, Z. CAI, S. G. VERMILYEA, E. PAPAZOGLOU, J. C. MITCHELL and A. B. CARR, *Cells Mater.* **6** (1996) 127.
5. T. K. VAIDYANATHAN and A. PRASAD, *J. Dent. Res.* **66** (1987) 205, Abstract No 786.
6. Z. CAI, W. A. BRANTLEY, A. B. CARR and J. C. MITCHELL, *ibid.* **72** (1993) 281, Abstract No 1421.
7. K. J. ANUSAVICE, C. SHEN, D. HASHINGER and S. W. TWIGGS, *ibid.* **64** (1985) 1094.
8. D. C. JACOVIDES, S. J. O'NEAL, W. R. LACEFIELD and R. C. COMPTON, *ibid.* **64** (1985) 246, Abstract No 639.
9. W. R. LACEFIELD, S. J. O'NEAL and H. K. COMPTON, *ibid.* **64** (1985) 246, Abstract No 640.
10. M. STAVRIDAKIS, E. PAPAZOGLOU, R. R. SEGHI, W. A. BRANTLEY and W. M. JOHNSTON, *ibid.* **76** (1997) 181, Abstract No 1339.
11. Z. CAI, X. CHU, S. D. BRADWAY, E. PAPAZOGLOU and W. A. BRANTLEY, *Cells Mater.* **5** (1995) 357.
12. W. A. BRANTLEY, Z. CAI, D. W. FOREMAN, J. C. MITCHELL, E. PAPAZOGLOU and A. B. CARR, *Dent. Mater.* **11** (1995) 154.
13. W. A. BRANTLEY, Z. CAI, Q. WU, A. B. CARR and J. C. MITCHELL, *Cells Mater.* **5** (1995) 261.
14. W. A. BRANTLEY, Z. CAI, J. C. MITCHELL and S. G. VERMILYEA, *ibid.* **7** (1997) 63.
15. Q. WU, W. A. BRANTLEY, S. G. VERMILYEA and J. C. MITCHELL, *J. Dent. Res.* **76** (1997) 79, Abstract No 528.
16. P. J. CASCONE, *ibid.* **63** (1984) 233, Abstract No 563.
17. W. A. BRANTLEY, Q. WU, Z. CAI, S. G. VERMILYEA and J. C. MITCHELL, *ibid.* **75** (1996) 60, Abstract No 339.
18. W. A. BRANTLEY, Q. WU, Z. CAI, S. G. VERMILYEA, J. C. MITCHELL and M. C. COMERFORD, *Cells Mater.* (in press).
19. ANSI/ADA specification no. 5 for dental casting alloys (Council on Dental Materials, Instruments and Equipment, Chicago, IL, USA, 1988).
20. ANSI/ADA specification no. 38 for metal-ceramic systems (Council on Dental Materials, Instruments and Equipment, Chicago, IL, USA, 1991).
21. K. ASGAR, B. TECHOW, F. C. ALLAN and L. V. SUTFIN, *J. Biomed. Mater. Res.* **3** (1969) 409.
22. H. M. YOUNG, R. MARGUELLES-BONNET and H. MOHAMMED, *Quint. Dent. Tech.* **11** (1987) 399.
23. W. J. PADILLA and R. W. RUDD, *J. Prosthet. Dent.* **76** (1996) 327.
24. H. MOHAMMED, M. A. HASSABALLA and Y. F. TALIC, *ibid.* **72** (1994) 433.
25. E. PAPAZOGLOU, W. A. BRANTLEY, A. B. CARR and W. M. JOHNSTON, *ibid.* **70** (1993) 386.
26. D. A. BRIDGEPORT, W. A. BRANTLEY and P. F. HERMAN, *J. Prosthod.* **2** (1993) 144.
27. ''Tensile testing.'' (ASM International, Metals Park, OH, USA, 1992), pp. 49–60.
28. G. E. DIETER in ''Mechanical Metallurgy'' (3rd ed, McGraw-Hill, New York, NY, USA, 1986) pp. 275–324 and 329–335.
29. L. L. LAUSTEN, N. H. LUEBKE and W. A. BRANTLEY, *J. Endodon.* **19** (1993) 440.
30. G. F. VANDER VOORT in ''Metallography: Principles and Practice'' (McGraw-Hill, New York, NY, USA, 1984) pp. 334–409 and 410–508.
31. Q. WU, W. A. BRANTLEY, J. C. MITCHELL, S. G. VERMILYEA, J. XIAO and W.GUO, *Cells Mater.* **7** (1997) 161.
32. Z. CAI, W. A. BRANTLEY, W. A. T. CLARK and H. O. COLIJN, *Dent. Mater.* **13** (1997) 365.
33. R. B. STEWART, K. GRETZ and W. A. BRANTLEY, *J. Dent. Res.* **71** (1992) 158, Abstract No 423.
34. M. H. REISBICK and W. A. BRANTLEY, *Int. J. Prosthodont.* **8** (1995) 346.

Received 7 September 1999
and accepted 13 December 1999